data while σ^{c}_{1ult} was adjusted to fit the calculated Tsai-Wu curve (dotted lines in Figure 4) well to the experimental strengths at $\alpha = 1/1$, 3/1 and 7/1. Therefore, the estimated compressive fatigue strength under cyclic loading is usually different from the tensile fatigue strength.

REFERENCES

1. 1991. *Fatigue of Composite Materials, Volume 4, Composite Materials Series*, K. L. Reifsnider, ed., Elsevier.
2. Owen, M. J. and J. R. Grifiths. 1978. "Evaluation of Biaxial Stress Failure Surfaces for a Glass Fabric Reinforced Polyester Resin under Static and Fatigue Loading," *J. of Materials Sci.*, 13:1521–1537.
3. Wang, S. S., E. S.-M. Chim and D. F. Socie. 1982. "Biaxial Fatigue of Fiber-Reinforced Composites at Cryogenic Temperatures. Part I: Fatigue Fracture Life and Mechanisms," *J. of Eng. Mate. and Tech., Trans. of ASME*, 104:128–136.
4. Krempel, E. and Niu, T. M. 1982. "Graphite/Epoxy $[\pm 45]_s$ Tubes. Their Static Axial and Shear Properties and Their Fatigue Behavior under Completely Reversed Load Controlled Loading," *J. of Composite Materials*, 16:172–187.
5. Krempel, E., D. M. Elzey, B. Z. Hong, T. Ayar and R. G. Loewy. 1988. "Uniaxial and Biaxial Fatigue Properties of Thin-Walled Composite Tubes," *J. of Am. Helicopter Soc.*, 33(3):3–10.
6. Amijima, S., T. Fujii and M. Hamaguchi. 1991. "Static and Fatigue Tests of a Woven Glass Fabric Composite under Biaxial Tension-Torsion Loading," *Composites*, 22(4):281–289.
7. Fujii, T., S. Amijima, T. Sagami and F. Lin. 1992. "Study on Strength and Nonlinear Stress-Strain Response of Plain Woven Glass Fiber Laminates under Biaxial Loading," *J. of Composite Mate.*, 26(17):2493–2510.
8. Amijima, S., T. Fujii and T. Sagami. 1991. "Nonlinear Behavior of Plain Woven G.F.R.P. under Repeated Biaxial Tension/Torsion Loading," *J. of Energy Resources Tech., Trans. of ASME*, 113:235–240.
9. Sines, G. and G. Ohgi. 1981. "Fatigue Criteria under Combined Stresses or Strains," *J. of Eng. Mate. and Tech., Trans. of ASME*, 103:82–90.
10. Fujczak, R. R. 1978. "Torsional Fatigue Behavior of Graphite-Epoxy Cylinders," *Proc. of ICCM II*, pp. 635–648.
11. Tsai, S. W. and E. M. Wu. 1971. "A General Theory of Strength for Anisotropic Materials," *J. Composite Mate.*, 5:58–80.
12. Amijima, S., T. Fujii and T. Sagami. 1989. "On the Strength and Stress-Strain Relations of Plain Woven Fiber Reinforced Plastics under Tension-Torsion Biaxial Loading," *J. of the Soc. of Mate. Sci. Japan*, 38(427):347–353.
13. Amijima, S. and T. Tanimoto. 1974. "On the Fatigue Properties of Glass Fiber Reinforced Plastics Subjected to Repeated Tension and Compression," *J. of the Soc. of Mate. Sci. Japan*, 23(250):581–587.
14. Fujii, T., S. Amijima and K. Okubo. 1993. "Microscopic Fatigue Progresses in a Plain-Woven Glass-Fibre Composite," *Composite Sci. and Tech.*, 49(4):327–333.
15. Nishitani, H., ed. 1985. *Hiro Kyodogaku* (Fatigue Strength of Materials) (in Japanese), Ohmu-sha (ISBN 4-274-08545-7), pp. 14–16.
16. Smith, E. W. and K. J. Pascoe. 1977. "The Role of Shear Deformation in Fatigue of a Glass Fiber-Reinforced Composite," *Composites*, 8:237–243.
17. Stinchcomb, W. W. and C. Bakis. 1991. "Fatigue Behavior of Composite Laminates," in *Fatigue of Composite Materials, Volume 4, Composite Materials Series*, K. L. Reifsnider, ed., Elsevier, pp. 105–180.

Interactive Buckling Analysis of Fiber-Reinforced Thin-Walled Columns

L. A. GODOY
Department of Civil Engineering
University of Puerto Rico at Mayaguez
Mayaguez, PR 00709

E. J. BARBERO AND I. RAFTOYIANNIS
Mechanical and Aerospace Engineering Department and
Constructed Facilities Center
West Virginia University
Morgantown, WV 26506-6106

(Received August 13, 1993)
(Revised March 4, 1994)

ABSTRACT: An analytical approximate model, leading to a closed form solution, is presented to account for buckling mode interaction in composite I section columns. Three buckling modes are considered in the analysis: a global mode (Euler mode about the weak axis); a primary local mode (rotation of the flanges and bending of the web); and a secondary local mode (bending of the flanges), which are modeled using analytical functions and four degrees of freedom. The fundamental state is shown to be linear and the three critical states for the isolated modes are found to be stable symmetric bifurcations. Mode interaction analysis in terms of the amplitudes of first order fields is carried out, for the first time, for prismatic sections of composite material. The tertiary (coupled) path involves coupling between the two local modes and it describes the sensitivity to imperfections of the buckling behavior of the composite column. A salient feature of the model presented is the closed form of the resulting solution, which enables the designer to easily perform parametric studies. Also, this is the first buckling mode interaction study for thin-walled composite columns. Numerical examples are presented to validate the results and to show the influence of the geometry and properties of the composite on the interaction phenomenon.

INTRODUCTION

FIBER REINFORCED PLASTIC (FRP) columns are used for civil engineering construction when corrosion resistance or electromagnetic transparency are required. Due to their light weight, thin-walled FRP and Metal Matrix Composite (MMC) sections are considered for space applications and as stiffeners for aircraft structures. In all these applications, the behavior under compressive loads may be very important.

0021-9983/95/05 591-23 $10.00/0

Recent studies (Barbero and Tomblin, 1992, 1993; Tomblin and Barbero, 1993) reported experimental procedures to determine: (a) local buckling behavior of the section, (b) global buckling loads, and (c) reduction of failure load in the intermediate region between short and long columns. Analytical models to predict the buckling loads of isolated modes (local and global) have been developed (Barbero and Raftoyiannis, 1993a, 1993b) and the predictions agree with the experimental data except in the intermediate region. It has been proposed that the reduction in failure load with respect to the isolated mode prediction may be caused by mode interaction. Whenever two modes are related to critical loads that are close, there is the possibility of having interaction between them leading to a new equilibrium path (a coupled path). Moreover, depending on the nature of the interaction, Supple (1967) found several possibilities, some of which are responsible for drastic reductions in the maximum loads that the system can attain.

A review of early work on interactive buckling may be found in the book by Thompson and Hunt (1973). Significant theoretical developments have been reported since then by Byskov and Hutchinson (1977), Hunt (1977), Reis (1977) and Maaskant (1989). There has been a renewed interest in the field in the last ten years, mainly in relation to the development of numerical methods. The application in the context of finite strip analysis has been pioneered by Sridharan and coworkers (see, for example, Benito and Sridharan, 1985a and 1985b; Sridharan and Ali, 1985; and Sridharan and Peng, 1989), and Mollmann and Goltermann (1989). Casciaro et al. studied interactive buckling between global (also called overall) and local modes in the context of finite elements (Casciaro et al., 1991). Kolakowski (1987, 1989, 1993) used analytical methods for the solution of trapezoidal columns. To the authors' best knowledge, the only prior studies related to buckling mode interaction in composite structures are those of Stoll (1993) and Sridharan and Starnes (1993).

Examples of interactive buckling in I section columns under axial load have been presented in the literature for isotropic materials. The interaction of a global and a local mode was considered in Sridharan and Benito (1984), and Benito and Sridharan (1985a and 1985b); they assumed a global mode and a local mode (associated to mode 2 in this paper) and by proposing a second order field, found a new mode containing only displacement in the flanges (mode 3 in this paper). A displacement containing first and second order fields proved to be imperfection sensitive. However, Sridharan and Ali (1985) found that the previous solution contained an error of unknown magnitude; thus they proposed to include the mode arising from the second order field as one of the principal modes participating in the interaction. Hence, the problem solved in Sridharan and Ali (1985, 1986) was interaction between a global, a primary local and a secondary local mode, in which only first order fields are included. Goltermann and Mollmann (1989) addressed the symmetric bending of an I beam, again using a three mode analysis based on the first order fields, but also included the influence of second order fields. The authors studied previously the two mode interaction of a primary local and a global mode; however, the analysis showed that if the modes are doubly symmetric then the second order contributions vanish and the first order interaction leads to an imperfection insensitive problem (Barbero, Raftoyiannis and Godoy, 1993).

All previous studies make use of numerical methods (finite strip or finite elements) and are oriented to metal structures, in which the material is assumed to be homogeneous. In the present work, a simplified model is presented, based on analytical functions, which can be applied to laminated, fiber reinforced composite materials. The general framework adopted is the theory of elastic stability for discrete systems, and the interactive buckling approach of Reis and Roorda (1979). Three modes are included in the analysis. It is shown that the resulting energy is doubly symmetric with respect to the global and primary local mode; however, it is not symmetric in the secondary local mode. Thus, the second order fields do not vanish and could be computed. However, the present analysis is restricted to the first order interaction, as in the works of Sridharan and Ali (1985).

DISPLACEMENT FIELD

Figure 1 shows the convention for local coordinates and displacements adopted in this work. The three modes considered in the analysis are depicted in Figure 2, and are represented in analytical form in this section. Figure 3 shows the degrees of freedom required to satisfy kinematic and compatibility requirements. A global mode is assumed to produce the following displacements in the web:

$$w_1^w = q_2 \sin\left(\frac{\pi x}{l}\right) \tag{1}$$

$$u_1^w = q_1 \frac{x}{l} \tag{2}$$

and in the flanges

$$v_1^f = q_2 \sin\left(\frac{\pi x}{l}\right) \tag{3}$$

$$u_1^f = q_1 \frac{x}{l} - \frac{\pi}{l} y q_2 \cos\left(\frac{\pi x}{l}\right) \tag{4}$$

The second term in u_1^f is a correction to account for Bernoulli hypothesis.

Next, a primary local mode is described by a rotation q_3 of the flanges and bending of the web as a plate. The displacements of the flanges are

$$w_2^f = y \sin q_3 \sin\left(\frac{n\pi x}{l}\right)$$

$$v_2^f = -y(1 - \cos q_3) \sin^2\left(\frac{n\pi x}{l}\right)$$

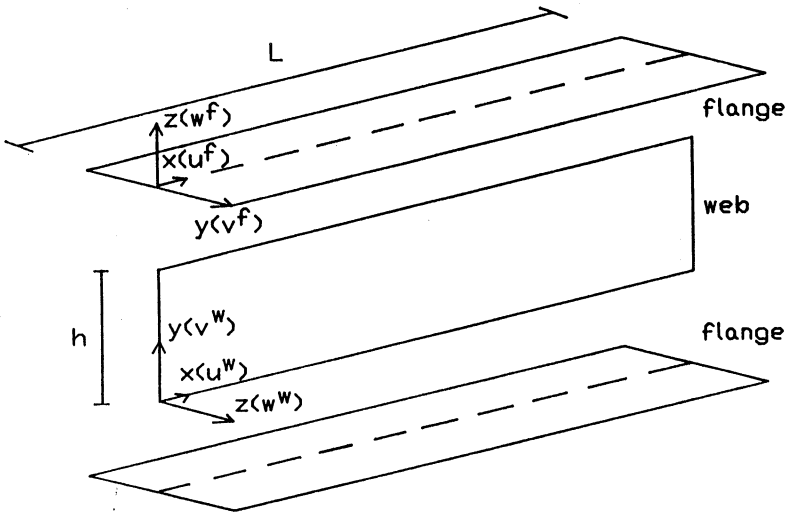

Figure 1. Convention adopted for local coordinates and displacements for each constituent plate.

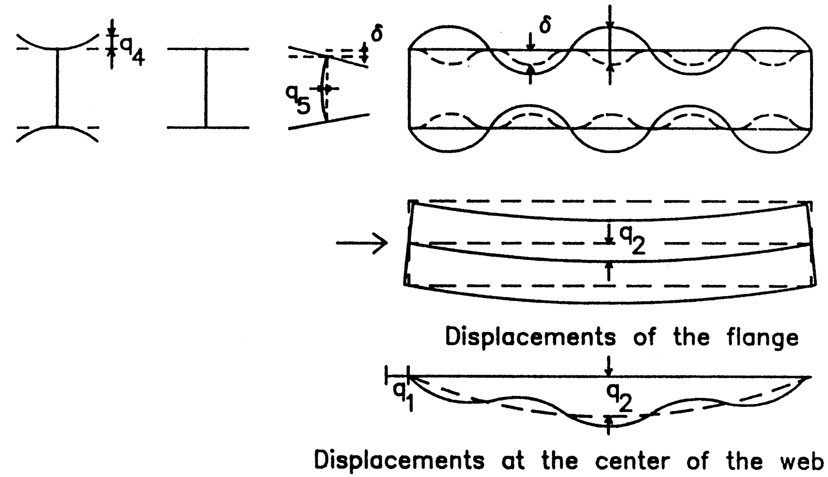

Figure 2. Local and global modes considered.

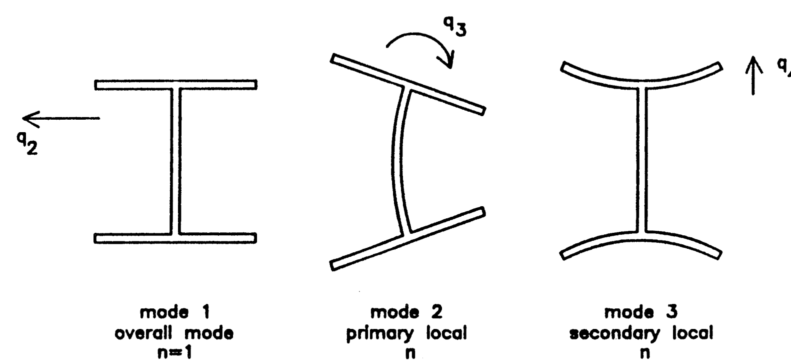

Figure 3. Displacement field assumed.

Expansion of the trigonometric functions in q_3 leads to

$$w_2^f = y \sin\left(\frac{n\pi x}{l}\right)\left(q_3 - \frac{q_3^3}{6}\right) \tag{5}$$

$$v_2^f = -\frac{1}{2} y q_3^2 \sin^2\left(\frac{n\pi x}{l}\right) \tag{6}$$

the displacements of the web due to a primary local mode are assumed as

$$w_2^w = f(y) q_5 \sin\left(\frac{n\pi x}{l}\right) \tag{7}$$

where the function employed to describe the variation of w^w with y is

$$f(y) = 4\left(\frac{y}{h} - \frac{y^2}{h^2}\right)$$

Finally, a secondary local mode is described in the form

$$w_3^f = q_4\left(\frac{2y}{b}\right)^2 \sin\left(\frac{n\pi x}{l}\right) \tag{8}$$

This is a local mode, with the same wavelength as the primary local mode, and is depicted in Figure 2. Benito and Sridharan (1985a, 1985b) identified this mode as the mixed second order field in a two-mode interaction analysis of an I column, and it was subsequently used by Sridharan and Ali (1985), and Benito and Sridharan (1985a, 1985b). Notice that this new mode does not introduce any displacements or rotations at the junction between web and flanges.

Compatibility of Rotations at the Junction

The degree of freedom q_5 has been assumed initially as independent of q_3; however they may be related if compatibility of rotations is enforced at the junction between the flanges and the web. The rotation from the web may be calculated as

$$\left.\frac{\partial w_2^w}{\partial y}\right|_{y=0} = q_5 \frac{4}{h} \sin\left(\frac{n\pi x}{l}\right)$$

The rotation of the flange is given by

$$\left.\frac{\partial w_2^f}{\partial y}\right|_{y=0} = \left(q_3 - \frac{1}{6} q_3^3\right) \sin\left(\frac{n\pi x}{l}\right)$$

for compatibility,

$$\left.\frac{\partial w_2^w}{\partial y}\right|_{y=0} = \left.\frac{\partial w_2^f}{\partial y}\right|_{y=0}$$

or else,

$$q_5 = \frac{h}{4}\left(q_3 - \frac{1}{6} q_3^3\right) \tag{9}$$

This represents a relation between q_5 and q_3 that can be substituted in w.

Compatibility of Vertical Displacements at the Junction

A displacement w_2^w produces a geometrical end-shortening of the web, δ, as indicated in Figure 2. This shortening may be calculated as

$$\delta = \frac{1}{2}\int_{y=0}^{h} \frac{1}{2}\left(\frac{\partial w_2^w}{\partial y}\right)^2 dy$$

Integrating and expanding

$$\delta = \frac{h}{12}\left(q_3^2 - \frac{1}{3} q_3^4\right) \sin^2\left(\frac{n\pi x}{l}\right) \tag{10}$$

Since for $y = 0$, $w_2^f = 0$, it is necessary to add δ to the displacement field of the flanges in order to satisfy compatibility of the vertical displacements.

Compatibility of Longitudinal Displacements

At the junction $y = 0$ both u_1^f and u_1^w have the same value; thus, compatibility is satisfied.

Compatibility of Horizontal Displacements

The horizontal displacements of the web are

$$\left. w^w \right|_{y=0} = \left. w_1^w + w_2^w \right|_{y=0} = q_2 \sin\left(\frac{\pi x}{l}\right)$$

At the flanges, one obtains

$$\left. v^f \right|_{y=0} = \left. v_1^f + v_2^f \right|_{y=0} = q_2 \sin\left(\frac{\pi x}{l}\right)$$

that satisfies compatibility.

Transverse Expansion of Flanges and Web

The large strains in the longitudinal direction produce a Poisson-type expansion of the flanges. If we consider that the N_y stress resultants in the flanges are zero (Barbero, Lopez-Anido, and Davalos, 1993), then

$$N_y = A_{12}^f \epsilon_x + A_{22}^f \epsilon_y = 0$$

or else

$$\epsilon_y = -\frac{A_{12}^f}{A_{22}^f}\epsilon_x \tag{11}$$

where the A_{ij}^f coefficients are defined in the constitutive relations of Equations (21). If only the linear part in ϵ_x is considered, then

$$\epsilon_y = -\frac{A_{12}^f}{A_{22}^f}\frac{\partial u_1^f}{\partial x} = -\frac{A_{12}^f}{A_{22}^f}\left(\frac{q_1}{l} + \frac{\pi^2 y}{l^2} q_2 \sin\left(\frac{\pi x}{l}\right)\right)$$

from which

$$v_3^f = \int_y \epsilon_y^f dy = -\frac{A_{12}^f}{A_{22}^f}\left(q_1\frac{y}{l} + \frac{\pi^2}{2l^2} y^2 q_2 \sin\left(\frac{\pi x}{l}\right)\right) \tag{12}$$

that should be added to the displacement field of the flanges. Something similar occurs in the web:

$$\epsilon_y = -\frac{A_{12}^w}{A_{22}^w}\frac{\partial u_1^w}{\partial x} = -\frac{q_1}{l}\frac{A_{12}^w}{A_{22}^w}$$

from which

$$v_3^w = -\frac{A_{12}^w}{A_{22}^w} q_1 \frac{\left|y - \frac{h}{2}\right|}{l} \tag{13}$$

Summary of Displacement Field

Adding the different contributions, the complete displacement field is obtained as

$$w^w = w_1^w + w_2^w, \quad u_w = u_1^w, \quad v^w = v_3^w$$

$$w^f = w_2^f - \delta_1, \quad u^f = u_1^f + u_3^f, \quad v^f = v_1^f + v_2^f + v_3^f$$

Substitution of each one of the components already calculated leads to a displacement field in terms of four degrees of freedom, with contributions from a global and two local modes of deformation.

In the web, these displacements are

$$w^w = q_2 \sin\left(\frac{\pi x}{l}\right) + h\left(\frac{y}{h} - \frac{y^2}{h^2}\right)\left(q_3 - \frac{q_3^3}{6}\right)\sin\left(\frac{n\pi x}{l}\right) \tag{14}$$

$$u^w = q_1\frac{x}{l} \tag{15}$$

$$v^w = -\frac{A_{12}^w}{A_{22}^w}\frac{\left|y - \frac{h}{2}\right|}{l} q_1 \tag{16}$$

while, for the flanges one may write

$$w^f = y\sin\left(\frac{n\pi x}{l}\right)\left(q_3 - \frac{q_3^3}{6}\right) - \frac{h}{12}\left(q_3^2 - \frac{q_3^4}{3}\right)\sin^2\left(\frac{n\pi x}{l}\right) + q_4\left(\frac{2y}{b}\right)^2\sin\left(\frac{n\pi x}{l}\right) \tag{17}$$

$$u^f = q_1\frac{x}{l} - y\frac{\pi}{l} q_2 \cos\left(\frac{\pi x}{l}\right) \tag{18}$$

$$v^f = q_2\sin\left(\frac{\pi x}{l}\right) - \frac{1}{2} y q_3^2 \sin^2\left(\frac{n\pi x}{l}\right) - \frac{A_{12}^f}{A_{22}^f}\left[q_1\frac{y}{l} + \frac{1}{2}\left(\frac{\pi y}{l}\right)^2 q_2 \sin\left(\frac{\pi x}{l}\right)\right] \tag{19}$$

TOTAL POTENTIAL ENERGY OF THE COLUMN

With the displacements field defined in Section 2, it is possible to obtain the membrane strains ϵ_x, ϵ_y and γ_{xy} and the changes in curvature χ_x, χ_y and χ_{xy} using the following nonlinear kinematic equations.

$$
\begin{aligned}
\epsilon_x &= \frac{\partial u}{\partial x} + \frac{1}{2}\left(\frac{\partial v}{\partial x}\right)^2 + \frac{1}{2}\left(\frac{\partial w}{\partial x}\right)^2 \\
\epsilon_y &= \frac{\partial v}{\partial y} + \frac{1}{2}\left(\frac{\partial u}{\partial y}\right)^2 + \frac{1}{2}\left(\frac{\partial w}{\partial y}\right)^2 \\
\gamma_{xy} &= \frac{\partial u}{\partial y} + \frac{\partial v}{\partial x} + \frac{\partial w}{\partial x}\frac{\partial w}{\partial y} \\
\chi_x &= -\frac{\partial^2 w}{\partial x^2} \\
\chi_y &= -\frac{\partial^2 w}{\partial y^2}
\end{aligned} \tag{20}
$$

$$\chi_{xy} = -2\frac{\partial^2 w}{\partial x \partial y}$$

Notice that these are not simply the von-Karman equations, but they also include the nonlinear terms in $\partial v/\partial x$ and $\partial u/\partial y$, as in the work of Benito and Sridharan (1985a, 1985b). These are necessary to represent correctly the nonlinearities, required for modal interaction analysis, at the junction of flange and web.

The general form of the constitutive equations, valid for a composite material with symmetric laminates, are next written as

$$\begin{aligned} N_x &= A_{11}\epsilon_x + A_{12}\epsilon_y \\ N_y &= A_{12}\epsilon_x + A_{22}\epsilon_y \\ N_{xy} &= A_{66}\gamma_{xy} \\ M_x &= D_{11}\chi_x + D_{12}\chi_y \\ M_y &= D_{12}\chi_x + D_{22}\chi_y \\ M_{xy} &= D_{66}\chi_{xy} \end{aligned} \tag{21}$$

where the membrane stress resultants are denoted by N_x, N_y and N_{xy}; the moment resultants are M_x, M_y and M_{xy}; and the constitutive coefficients for a composite material are readily obtained in the literature (Jones, 1975; Tsai, 1989). The strain energy of the web may be written as

$$U^{web} = U_m^{web} + U_b^{web} \tag{22}$$

where

$$U_m^{web} = \frac{1}{2}\int_{x=0}^{l}\int_{y=0}^{h}(N_x\epsilon_x + N_y\epsilon_y + N_{xy}\gamma_{xy})dxdy$$

$$U_b^{web} = \frac{1}{2}\int_{x=0}^{l}\int_{y=0}^{h}(M_x\chi_x + M_y\chi_y + M_{xy}\chi_{xy})dxdy$$

The strain energy stored due to deformation of the two flanges is

$$U^{fl} = 2(U_m^{fl} + U_b^{fl}) \tag{23}$$

where

$$U_m^{fl} = \frac{1}{2}\int_{x=0}^{l}\int_{y=-b/2}^{b/2}(N_x\epsilon_x + N_y\epsilon_y + N_{xy}\gamma_{xy})dxdy$$

$$U_b^{fl} = \frac{1}{2}\int_{x=0}^{l}\int_{y=-b/2}^{b/2}(M_x\chi_x + M_y\chi_y + M_{xy}\chi_{xy})dxdy$$

Finally, the load potential is computed as

$$\Omega = +Pq_1 \tag{24}$$

The total potential energy V is next obtained by adding Equations (22–24) in the form

$$V = U^{web} + U^{fl} - \Omega \tag{25}$$

An explicit form of V in terms of the degrees of freedom q_i has been obtained with the aid of the algebraic symbolic manipulator Maple V (Char et al., 1991). A convenient form to write the resulting energy in terms of discrete generalized coordinates q_i is to express it as the Taylor expansion:

$$V[q_i,\Lambda] = \Lambda\hat{V}_i' q_i + \frac{1}{2}\hat{V}_{ij}q_iq_j + \frac{1}{3!}\hat{V}_{ijk}q_iq_jq_k + \frac{1}{4!}\hat{V}_{ijkl}q_iq_jq_kq_l \tag{26}$$

for $i, j, k, l = 1,\ldots,4$. It is important to notice that the coefficients are symmetric, and the only non-zero values are

$$\hat{V}_1', \hat{V}_{11}, \hat{V}_{22}, \hat{V}_{33}, \hat{V}_{44}, \hat{V}_{122}, \hat{V}_{133}, \hat{V}_{144}, \hat{V}_{234}$$

$$\hat{V}_{334}, \hat{V}_{2222}, \hat{V}_{3333}, \hat{V}_{4444}, \hat{V}_{1334}, \hat{V}_{2233}, \hat{V}_{2244}, \hat{V}_{3344}$$

FUNDAMENTAL PATH AND DISTINCT CRITICAL STATES

The fundamental path is obtained from the equilibrium condition $V_i = 0$, where $(\,)_i$ denotes a derivative with respect to the q_i degree of freedom. In the present case only the first equation is relevant, leading to the linear fundamental path

$$Q^F = \{\bar{Q}_1, 0, 0, 0\} \tag{27}$$

where

$$q_1 = \bar{Q}_1\Lambda = -V_1/V_{11},\ q_i = 0 \text{ if } i \neq 1$$

In the following we use the W-formulation where the energy is written in terms of incremental displacements. This is a simplification with respect to the V-formulation where the energy is written in terms of total displacements. However, the use of the W-formulation does not introduce any new approximation to the problem. Note that the same notation (q_i) is used for the total and incremental displacements. Only the end-shortening of the column is different (by the additive term $\bar{Q}_1\Lambda$) when measured in total or incremental displacement.

Furthermore, once the problem is cast in the W-formulation, the end-shortening q_1 disappears from the analysis. The remaining generalized coordinates q_2, q_3, q_4, are identical when measured as total or incremental displacements. Next, q_1 is substituted by $\bar{Q}_1\Lambda + q_1$ into V to compute the energy in terms of the incremental displacements q_i. The condition of critical state takes the form

$$(\hat{V}_{ij} + \Lambda^s \hat{V}_{ijk}\bar{Q}_k)\, x_j^s |^c = 0 \tag{28}$$

where there is no summation in s, Λ^s is the s-eigenvalue representing the critical load of the system, and x_j^s are the associated eigenvectors (isolated modes).

Because of the diagonal form of the coefficients, the eigenvalues result in

$$\Lambda_c^1 = -\frac{\hat{V}_{22}}{\hat{V}_{221}\bar{Q}_1}, \quad \Lambda_c^2 = -\frac{\hat{V}_{33}}{\hat{V}_{331}\bar{Q}_1}, \quad \Lambda_c^3 = -\frac{\hat{V}_{44}}{\hat{V}_{441}\bar{Q}_1} \tag{29}$$

The eigenvectors x_j^s are normalized so that they satisfy the condition (Reis and Roorda, 1979)

$$\hat{V}_{ijk}\bar{Q}_k x_j^s x_i^t = \delta_{st}$$

leading to

$$\begin{aligned} x^1 &= \{0, (\hat{V}_{221}\bar{Q}_1)^{-1/2}, 0, 0\} \\ x^2 &= \{0, 0, (\hat{V}_{331}\bar{Q}_1)^{-1/2}, 0\} \\ x^3 &= \{0, 0, 0, (\hat{V}_{441}\bar{Q}_1)^{-1/2}\} \end{aligned} \tag{30}$$

The three critical states are bifurcations (since $V_i x_i^s|^c = 0$) and represent symmetric bifurcations (since $V_{ijk} x_i^s x_j^s x_k^s|^c = 0$). Using the general theory of elastic stability (Thompson and Hunt, 1973; Flores and Godoy, 1992) it is possible to show that all three bifurcations are stable, thus leading to rising paths with positive curvature. If the eigenvalues of Equations (29) are well apart from each other, it is possible to load the column up to the lowest critical load Λ_c^s ($s = 1.3$) and no modal interaction is present. Notice that the proximity between different eigenvalues depends on the geometry of the system and the constitutive coefficients of the composite material.

MODE INTERACTION

The mode interaction analysis is carried out here within the context of the works of Reis (1977) and Reis and Roorda (1979). With three modes included in the interactive analysis, it is possible to consider the incremental displacements q_i in the form

$$q_i = x_i^s \xi_s \qquad s = 1, 2, 3 \tag{31}$$

where ξ_s are the modal amplitudes of the displacement in the so-called first order field (Benito and Sridharan, 1985a, 1985b). Notice that second order fields (having $\xi_s\xi_t x_i^{st}$, where x_i^{st} are new modes emerging from the interaction) have not been included in Equation (31). The reason for this is that mode 3 is the new mode that would arise from a 2-mode analysis, and it has now been included as a competing mode in the linear combination of Equation (31). A similar analysis is discussed in Goltermann and Mollmann (1989).

Substitution of Equation (31) into the total potential energy leads to a new functional W in terms of the modal amplitudes ξ_s as

$$\begin{aligned} W[\xi_1, \xi_2, \xi_3, \Lambda] &= \frac{1}{2}(\Lambda - \Lambda_c^1)\xi_1^2 + \frac{1}{2}(\Lambda - \Lambda_c^2)\xi_2^2 + \frac{1}{2}(\Lambda - \Lambda_c^3)\xi_3^2 \\ &+ b_{123}\xi_1\xi_2\xi_3 + b_{223}\xi_2^2\xi_3 + c_{1111}\xi_1^4 + c_{2222}\xi_2^4 \\ &+ c_{3333}\xi_3^4 + c_{1122}\xi_1^2\xi_2^2 + c_{1133}\xi_1^2\xi_3^2 + c_{2233}\xi_2^2\xi_3^2 \end{aligned} \tag{32}$$

where

$$b_{123} = \hat{V}_{234} x_2^1 x_3^2 x_4^3$$

$$b_{223} = \frac{1}{2}(\hat{V}_{334} + \Lambda \hat{V}_{1334}\bar{Q}_1)(x_3^2)^2 x_4^3$$

$$c_{1111} = \frac{1}{24}\hat{V}_{2222}(x_2^1)^4$$

$$c_{2222} = \frac{1}{24}\hat{V}_{3333}(x_3^2)^4$$

$$c_{3333} = \frac{1}{24}\hat{V}_{4444}(x_4^3)^4$$

$$c_{1122} = \frac{1}{4}\hat{V}_{2233}(x_2^1)^2(x_3^2)^2$$

$$c_{2233} = \frac{1}{4} \hat{V}_{3344}(x_3^3)^2(x_4^3)^2$$

$$c_{1133} = \frac{1}{4} \hat{V}_{2244}(x_2^1)^2(x_4^3)^2$$

Notice that the only load-dependent coefficient is b_{223}. The following properties of symmetry of the modes are detected in W:

$$\begin{aligned} W[-\xi_1, -\xi_2, \xi_3, \Lambda] &= W[\xi_1, \xi_2, \xi_3, \Lambda] \\ W[-\xi_1, \xi_2, -\xi_3, \Lambda] &\neq W[\xi_1, \xi_2, \xi_3, \Lambda] \\ W[\xi_1, -\xi_2, -\xi_3, \Lambda] &\neq W[\xi_1, \xi_2, \xi_3, \Lambda] \end{aligned} \tag{33}$$

that is, the energy is doubly symmetric with respect to the global and primary local mode but it is not symmetric with respect to the secondary local mode.

Equilibrium Paths

Three equilibrium conditions are obtained from the first derivatives of Equation (32) with respect to the ξ_s, and they are

$$\begin{aligned} &(\Lambda - \Lambda_c^1)\xi_1 + b_{123}\xi_2\xi_3 + 4c_{1111}\xi_1^3 + 2c_{1122}\xi_1\xi_2^2 + 2c_{1133}\xi_1\xi_2^2 = 0 \\ &(\Lambda - \Lambda_c^2)\xi_2 + b_{123}\xi_1\xi_3 + 4c_{2222}\xi_2^3 + 2c_{2233}\xi_2\xi_3^2 + 2c_{1122}\xi_1^2\xi_2 + 2b_{223}\xi_2\xi_3 = 0 \\ &(\Lambda - \Lambda_c^3)\xi_3 + b_{123}\xi_1\xi_2 + 4c_{3333}\xi_3^3 + 2c_{1133}\xi_1^2\xi_3 + 2c_{2233}\xi_2^2\xi_3 + b_{223}\xi_2^2 = 0 \end{aligned} \tag{34}$$

The solution $\xi_s = 0$ for $s = 1,2,3$ satisfies Equation (34) and is the fundamental path in the $\xi_s - \Lambda$ space. The secondary path for the isolated mode Λ_c^s is obtained by considering $\xi_s \neq 0$ and the other two amplitudes equal to zero, in which case the s-equilibrium equation leads to

$$\xi_s[(\Lambda - \Lambda_c^s) + 4c_{ssss}\xi_s^2] = 0 \tag{35}$$

(no summation in s)

Since all c_{ssss} coefficients are positive, the path emerging from Λ_c^s is stable symmetric. The solutions with $\xi_s \neq 0$ ($s = 1,2,3$) represent the coupled paths resulting from interaction between modes. They are three cubic equations; however it is possible to obtain a quadratic approximation from the following system.

$$(\Lambda - \Lambda_c^1)\xi_1 + b_{123}\xi_2\xi_3 = 0 \tag{36a}$$

$$(\Lambda - \Lambda_c^2)\xi_2 + b_{123}\xi_1\xi_3 + 2b_{223}\xi_2\xi_3 = 0 \tag{36b}$$

$$(\Lambda - \Lambda_c^3)\xi_3 + b_{123}\xi_1\xi_2 + b_{223}\xi_2^2 = 0 \tag{36c}$$

From Equation (36a), ξ_1 is obtained as a function of ξ_2, ξ_3 and then substituted into (36b), leading to

$$\xi_2[\alpha_3\xi_3^2 + \beta_3\xi_3 + \gamma_3] = 0 \tag{37}$$

where

$$\alpha_3 \equiv -\frac{(b_{123})^2}{\Lambda - \Lambda_c^1}, \ \beta_3 \equiv 2b_{223}, \ \gamma_3 \equiv \Lambda - \Lambda_c^2$$

From Equation (37), ξ_3 results as

$$\xi_3 = \frac{-\beta_3 \pm \sqrt{\beta_3^2 - 4\alpha_3\gamma_3}}{2\alpha_3} \tag{38}$$

Finally, from Equation (36c) the following condition is obtained by substitution of ξ_1 and ξ_3:

$$\alpha_2\xi_2^2 + \gamma_2 = 0 \tag{39}$$

where

$$\alpha_2 \equiv b_{223} - (b_{123})^2 \frac{\xi_3}{\Lambda - \Lambda_c^1}, \ \gamma_2 \equiv (\Lambda - \Lambda_c^3)\xi_3$$

Thus, ξ_2 results in the form

$$\xi_2^2 = -\frac{\gamma_2}{\alpha_2} \tag{40}$$

with ξ_1 given by

$$\xi_1 = \gamma_1 = -b_{123}\frac{\xi_2\xi_3}{\Lambda - \Lambda_c^1} \tag{41}$$

The values of ξ_1, ξ_2 and ξ_3 from Equations (38), (40), and (41) may be substituted into Equation (31) leading to a coupled path in the form

$$q = \{0, 0, x_3^2\xi_2, x_4^3\xi_3\} \tag{42}$$

This is a tertiary path that arises as a consequence of the interaction between the two local modes.

RESULTS

The model presented has been validated for I columns made of homogeneous materials by comparisons with results obtained by Benito and Sridharan (1985a). Furthermore, a finite element code is being developed by the authors for instability of plate assemblies made of composite materials (Godoy, Barbero and Raftoyiannis, 1993) and some comparisons for isolated modes are presented in this section.

First, let us consider a column with the geometry defined by $b = 6$ in; $h = 6$ in; and material properties for the flanges given by $A_{11} = 893{,}500$ lb-in; $A_{22} = 343{,}000$ lb-in; $A_{12} = 130{,}800$ lb-in; $A_{66} = 113{,}600$ lb-in; $D_{11} = 4{,}289$ lb-in; $D_{22} = 2{,}029$ lb-in; $D_{12} = 807.3$ lb-in; and $D_{66} = 641.5$ lb-in. For the web, the properties are $D_{11} = 4{,}090$ lb-in; $D_{22} = 1{,}863$ lb-in; $D_{12} = 731.6$ lb-in; and $D_{66} = 596.1$ lb-in. These properties correspond to a $6 \times 6 \times 1/4$ in. pultruded WF-beam (Creative Pultrusions, 1989). The length has been chosen so that the two lowest critical loads are almost coincident. = 100

The fundamental path is $\bar{Q}_1\Lambda$, with $\bar{Q}_1 = 0.658537 \times 10^{-5}$, with the critical loads given by Equation (29) as $\Lambda_c^1 = 30{,}021.9$ lb (global); $\Lambda_c^2 = 28{,}633.7$ lb (primary local); and $\Lambda_c^3 = 142{,}422.6$ lb (secondary local load). The associated eigenvectors, Equation (30), are

$x^1 = \{0, 4.5, 0, 0\}$: global mode

$x^2 = \{0, 0, 0.322, 0\}$: primary local mode

$x^3 = \{0, 0, 0, 1.369\}$: secondary local mode

The finite element model developed by the authors (see Godoy et al., 1993) yields values of critical loads of $\Lambda_c^2 = 27{,}375$ lb for the primary local load; and $\Lambda_c^1 = 29{,}776$ lb for the global mode. The eigenvector of the primary local mode in the F. E. analysis is slightly different from the one assumed in the present model, in the sense that the flanges not only rotate but also show some bending. Bending of the flanges is incorporated in the present model into the secondary local mode. The largest displacement component in the eigenvectors calculated with finite elements are 4.48, 0.558 and 1.369 for the global, primary local, and secondary local modes respectively. The global mode is in good agreement with the present calculations (4.5); the differences in the local modes (0.322, 1.369) are caused by slight bending of the flanges.

For the isolated modes, the post-buckling path is stable and the curvature of the primary local mode, obtained using the general theory of elastic stability (Thompson and Hunt, 1973), is 215,222; while a value of 160,406 is obtained in the F. E. analysis. The differences between these are caused by slightly different boundary conditions used in the F. E. model. The present analytical model satisfies simply supported conditions at the ends, while in the finite element model the end section may deform freely away from the Bernoulli assumptions. These differences in curvature due to the boundary conditions have been observed previously by Sridharan and Graves Smith (1978).

Results of the post-critical path in terms of the mode amplitude ξ_1 [Equations (41–42)] are presented in Figure 4. In the present analysis, ξ_1 is coincident with the coordinate q_3; ξ_2 with q_2; and ξ_3 with q_4. The amplitude in the primary local mode q_3 is plotted in Figure 4 versus the load. A secondary path with positive curvature is stable, with the branch going up with the load. The tertiary path resulting from mode interaction is unstable, with the branch going down with the load, which is indicative of an imperfection sensitive structure. In the present problem, the tertiary path has components in ξ_1 and ξ_3, starts at a new critical state, and falls to lower values of the load with increasing displacements. This new path is characteristic of imperfection sensitive structures, and should be of great concern to the designer for this particular geometry, in which the modes are likely to interact.

To investigate the influence of the material properties of the composite on the coefficients of the nonlinear Equations (36) and (42), it is convenient to define the ratio $r = A_{22}/A_{11}$. This ratio reflects the relative membrane stiffness between the transverse and the axial directions in the column. It is assumed that the bending relations are also given by r, so that $D_{22} = rD_{11}$. In the case studied in Figure 4, the value of r is 1/3. The coefficients b_{223} and b_{123} are the only nonvanishing coefficients governing the shape of the tertiary path (interactive mode) of the column. Therefore, the variation of these coefficients with the material properties is very important. The coefficients b_{223} and b_{123} are plotted in Figures 5a and 5b as

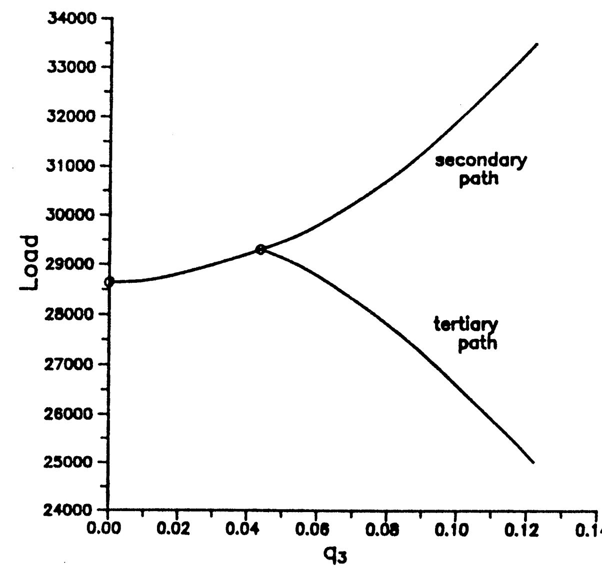

Figure 4. *Secondary and tertiary path for a section with b = h = 6 in; L = 100 in. Equilibrium paths in terms of the amplitude of the primary local mode.*

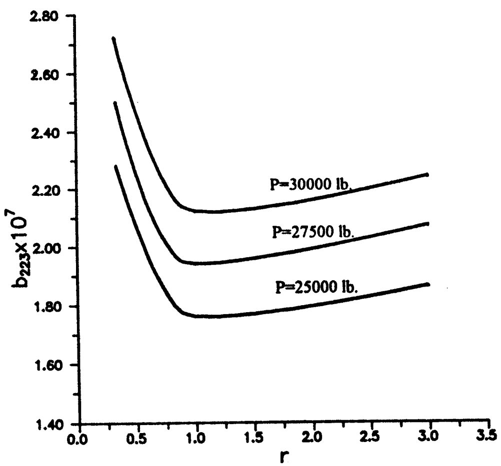

Figure 5a. *Influence of the material properties of the composite,* r = A_{22}/A_{11}, *on the quadratic coefficient* b_{223}.

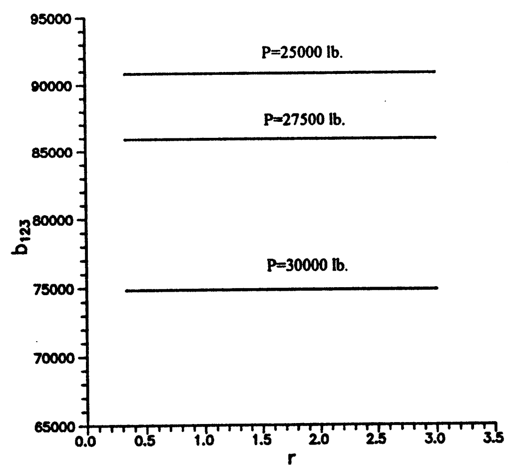

Figure 5b. *Influence of the material properties of the composite,* r = A_{22}/A_{11}, *on the quadratic coefficient* b_{123}.

a function of r. When the material properties change, different lengths have to be considered to obtain almost coincidence between the primary local and the global critical loads. Therefore, the following column lengths are used: $L = 100$ in. for $r = 1/3$, $L = 82$ in. for $r = 1$, and $L = 60$ in. for $r = 3$. The corresponding global critical loads are 30,021 lb, 31,349 lb, and 30,020 lb. It may be seen in Figure 5a that b_{223} displays a minimum value for $r = 1$, that is, the homogeneous material; while b_{123} shown in Figure 5b. is constant with r. Since the coefficient b_{223} depends on the applied load, three curves are shown in Figure 5a for loads in the range of interest, that is for values less than or equal to the global critical load. It is clear that the variation of the coefficients b_{223} and b_{123} is similar for different load levels.

Finally, results are presented in Figures 6a and 6b for the tertiary path as a function of r, with values $r = 1/3, L = 100$ in.; $r = 1, L = 82$ in.; and $r = 3$, $L = 60$ in. Once again, the tertiary path, originated as a result of mode interaction, is unstable as shown in Figure 6a for the $\Lambda - q_3$ plane, even though the projection on the $\Lambda - q_4$ plane, shown in Figure 6b, seems flat. The curvature of the tertiary path, which is indicative of the sensitivity to imperfection, changes with the material properties (ratio r) as a result of changes in the coefficient b_{223}.

The material properties play an important role in the interactive buckling of the I column. Conversely, it is possible to design the material properties so as to

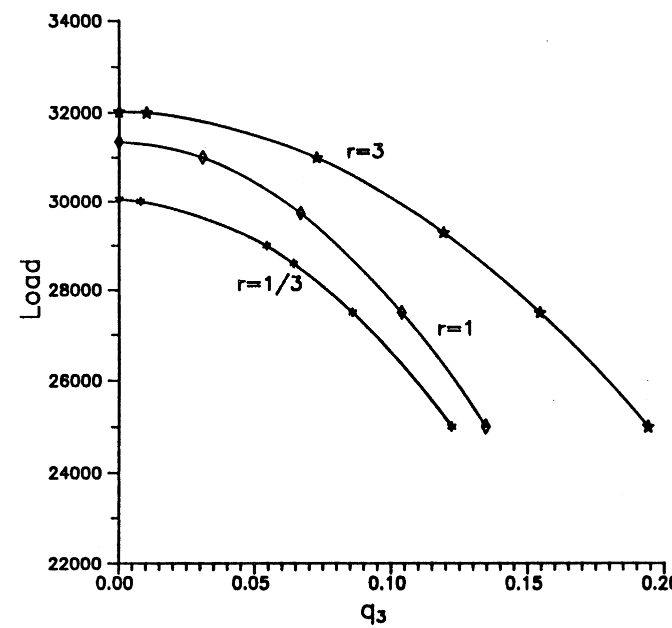

Figure 6a. *Influence of the material properties of the composite,* r = A_{22}/A_{11}, *on the tertiary path.*

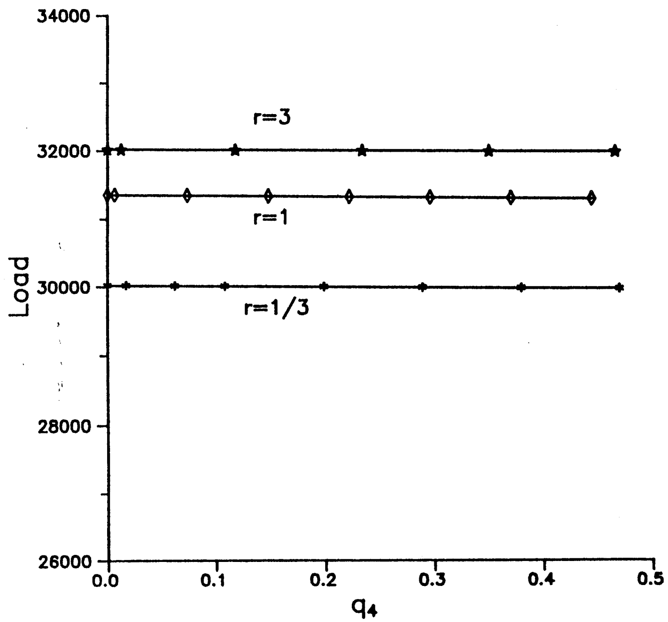

Figure 6b. *Influence of the material properties of the composite,* r = A_{22}/A_{11}, *on the tertiary path.*

avoid the occurrence of interaction for a given length. This is not possible in homogeneous sections, and is one of the advantages of using composite materials.

CONCLUSIONS

An analytical solution for the interactive analysis of composite I columns has been presented, in which the cooperation of all the walls of the structure is considered. The framework of the analysis is the general theory of elastic stability.

The main hypotheses concerning the structure are uniform compression at the ends of the column; simply supported boundary conditions; and that the flanges and the web can freely expand in transverse direction to the applied load. The displacement field assumed satisfies compatibility conditions at the junctions between web and flanges. Local modes are assumed to have a constant maximum amplitude in the longitudinal direction: this is not entirely correct, as demonstrated by Koiter, and an effect of amplitude modulation should be included in a more refined model. Sridharan and Ali (1985) have included this effect into a finite element analysis. The more detailed finite element code for composite structures developed by the authors (Godoy et al., 1993) takes such modulation of amplitude into account automatically. In the present work, the resulting energy has four degrees of freedom and is quartic; it requires eight coefficients to model

the properties of the composite material, namely A_{11}, A_{22}, A_{12}, A_{66}, D_{11}, D_{22}, D_{12} and D_{66}. The fundamental path is linear, with the quadratic form of the energy (second variation along the fundamental path) being diagonal, the system leads to three isolated critical states that are stable symmetric bifurcations. Mode interaction is based on a three mode analysis, and considered in terms of the so-called first order fields (a linear contribution of the three isolated modes, in which the coefficients of the contribution are load dependent). The coupled path is evaluated from a quadratic approximation to the equilibrium condition.

Since there is no previous work in this field reported in the literature, the only numerical validation of the procedure was performed for uncoupled paths and using a finite element solution developed by the authors. It is expected to further validate these results against new experimental work and also against numerical results from the finite element model extended to account for interactive buckling.

Concerning the application to composite materials, it is possible to say that the model takes into account symmetric laminates. One of the advantages of the present approach is that results can be obtained using a personal computer and are computationally inexpensive; thus, parametric studies changing the material properties, to obtain an optimum in terms of both cost and safety, are simple to be carried out. Thus, it is expected that the model could be used as a useful tool for the design of pultruded columns.

ACKNOWLEDGEMENTS

L. Godoy was on leave from the National University of Cordoba and the Science Council of Argentina during the period of this research. This project was partially sponsored by NSF Grant 8802265 and West Virginia Department of Highways Grant RPT699. The financial support is gratefully acknowledged. We recognize Dr. Hota V. S. Ganga Rao, Director, Constructed Facilities Center, for his help and comments about this work.

REFERENCES

Ali, A. and S. Sridharan. 1989. "A Special Beam Element for the Analysis of Thin-Walled Structural Components," *Int. J. Numerical Methods in Engineering*, 28:1733–1747.

Barbero, E. J., R. Lopez-Anido and J. Davalos. 1993. "On the Mechanics of Thin-Walled Laminated Composite Beams," *J. Composite Materials*, 27(8):806–829.

Barbero, E. J., I. G. Raftoyiannis and L. A. Godoy. 1993. "Mode Interaction in FRP Columns," in *Mechanics of Composite Materials: Non-Linear Effects*, M. H. Hyer, ed., AMD, vol. 159, New York: American Society of Mechanical Engineers, pp. 9–18.

Barbero, E. J. and I. G. Raftoyiannis. 1993a. "Local Buckling of FRP Beams and Columns," *ASCE J. of Materials in Civil Engineering*, 5(3):339–355.

Barbero, E. J. and I. G. Raftoyiannis. 1993b. "Euler Buckling of Pultruded Composite Columns," *Composite Structures Int. Journal*, 24:139–147.

Barbero, E. J. and J. Tomblin. 1992. "Euler Buckling of Thin Walled Composite Columns," *AIAA Journal*, 30(11):2798–2800.

Barbero, E. J. and J. Tomblin. 1994. "A Phenomenologic Design Equation for FRP Columns with Interaction between Local and Global Buckling," *Thin-Walled Structures*, 18:117–131.

Benito, R. and S. Sridharan. 1985a. "Interactive Buckling Analysis with Finite Strips," *Int. J. Numerical Methods in Engineering*, 21:145–161.

Benito, R. and S. Sridharan. 1985b. "Mode Interaction in Thin-Walled Structural Members," *J. Structural Mechanics*, ASCE, 12(4):517–542.

Byskov, E. and J. Hutchinson. 1977. "Mode Interaction in Axially Stiffened Cylindrical Shells," *AIAA Journal*, 15(7):941–948.

Casciaro, R., A. D. Lanzo and G. Salerno. 1991. "Computational Problems in Elastic Structural Stability," in *Non-Linear Problems in Engineering*, C. Carmignani and G. Maino, eds., New Jersey: World Scientific, pp. 66–83.

Char, B. W. et al. 1991. *Maple V Language Reference Manual.* New York: Springer-Verlag.

Creative Pultrusions Inc. 1989. *Design Guide.* Alum Bank, PA.

Flores, F. and L. Godoy. 1992. "Elastic Postbuckling Analysis via Finite Element and Perturbation Techniques, Part I: Formulation," *Int. J. Num. Methods in Engng.*, 33:1775–1794.

Godoy, L., E. Barbero and I. Raftoyiannis. 1993. "Finite Elements for Post-Buckling Analysis: Part 1, The W-Formulation," *Computers and Structures*, in press.

Goltermann, P. and H. Mollmann. 1989. "Interactive Buckling in Thin-Walled Beams. II Applications," *Int. J. Solids and Structures*, 25(7):729–749.

Graves Smith, T. R. and S. Sridharan. 1978. "A Finite Strip Method for the Post-Locally Buckled Analysis of Plate Structures," *Int. J. Mechanical Sciences*, 20:833–842.

Hunt, G. W. 1977. "Imperfection Sensitivity of Semi-Symmetric Branching," *Proc. Royal Soc. of London, Ser. A.*, 357:193.

Jones, R. M. 1975. *Mechanics of Composite Materials.* New York: Hemisphere Publishing Co.

Koiter, W. T. 1976. "General Theory of Mode Interaction in Stiffened Plate and Shell Structures," Report No. 590, Delft University of Technology, Delft, The Netherlands.

Kolakowski, Z. 1987. "Mode Interaction in Thin-Walled Trapezoidal Column under Uniform Compression," *Thin-Walled Structures*, 5:329–342.

Kolakowski, Z. 1989. "Some Thoughts on Mode Interaction in Thin-Walled Columns under Uniform Compression," *Thin-Walled Structures*, 7:23–35.

Kolakowski, Z. 1993. "Interactive Buckling of Thin-Walled Beam-Columns with Open and Closed Cross Sections," *Thin-Walled Structures*, 15:159–183.

Maaskant, R. 1989. "Interactive Buckling of Biaxially Loaded Elastic Plate Structures," Ph.D. Thesis, University of Waterloo, Ontario, Canada.

Mollmann, H. and P. Goltermann. 1989. "Interactive Buckling in Thin-Walled Beams. I Theory," *Int. J. Solids and Structures*, 25(7):715–728.

Pignataro, M., A. Luongo and N. Rizzi. 1985. "On the Effect of the Local Overall Interaction on the Postbuckling of Uniformly Compressed Channels," *Thin-Walled Structures*, 3:293–321.

Reis, A. J. and J. Roorda. 1979. "Post-Buckling Behavior under Mode Interaction," *J. of Eng. Mech. Division*, ASCE, 105(EM4):609–621.

Reis, A. J. 1977. "Interactive Buckling in Elastic Structures," Ph.D. Thesis, University of Waterloo, Ontario, Canada.

Reis, A. J. 1987. "Interactive Buckling of Thin-Walled Structures," in *Developments in Thin-Walled Structures, Vol. 3*, J. Rhodes and A. C. Walker, eds., London: Elsevier Applied Science Publ., pp. 237–279.

Sridharan, S. and A. Ali. 1985. "Interactive Buckling in Thin-Walled Beam-Columns," *J. Engineering Mechanics*, ASCE, 111(12):1470–1486.

Sridharan, S. and A. Ali. 1986. "An Improved Interactive Buckling Analysis of Thin-Walled Columns Having Doubly Symmetric Cross-Sections," *Int. J. Solids and Structures*, 22(4):429–443.

Sridharan, S. and R. Benito. 1984. "Columns: Static and Dynamic Interactive Buckling," *Journal of Engineering Mechanics*, ASCE, 110(1):49–65.

Sridharan, S. and T. H. Starnes, Jr. 1993. "Mode Interaction in Stiffened Composite Panels," *First Joint Meeting SES-ASCE-ASME*, Charlottesville, VA, June 6–9.

Stoll, F. 1993. "Analysis of Non-Linear Response of Compressive Loaded Stiffened Panels," *First Joint Meeting SES-ASCE-ASME*, Charlottesville, VA, June 6–9.

Supple, W. 1967. "Coupled Branching Configurations in the Elastic Buckling of Symmetric Structural Systems," *Int. J. Mech. Sci.*, 9:97–112.

Thompson, J. M. and G. W. Hunt. *A General Theory of Elastic Stability.* New York: John Wiley and Sons.

Tomblin, J. and E. J. Barbero. 1994. "Local Buckling Experiments on FRP Columns," *Thin-Walled Structures*, 18:97–116.

Tsai, S. W. 1989. *Composites Design, 4th Ed.* New York: Think Composites.